Quantum fractal superlattices

Juan A. Monsoriu[a)]
Departamento de Física Aplicada, Universidad Politécnica de Valencia, E-46022 Valencia, Spain

Francisco R. Villatoro
Departamento de Lenguajes y Ciencias de la Computación, Universidad de Málaga, E-29071 Málaga, Spain

María J. Marín
Departamento de Termodinámica, Universitat de València, E-46100 Burjassot, Spain

Jezabel Pérez
Departamento de Matemática Aplicada, Universidad Politécnica de Valencia, E-46022 Valencia, Spain

Llúcia Monreal
Departamento de Matemática Aplicada, Universidad Politécnica de Valencia, E-46022 Valencia, Spain

(Received 11 October 2005; accepted 5 May 2006)

Fractal superlattices consist of a series of thin layers of two semiconductor materials alternately deposited on each other with widths corresponding to the rules of construction of a fractal set. The scattering of electrons in superlattices is obtained using the transfer matrix method for generalized Cantor fractal potentials that are characterized by a lacunarity parameter. The numerical results show the self-similarity of the reflection coefficient and the appearance of lacunarity-independent energies with perfectly transparent tunneling due to the bound states of the particle in each of the individual potential wells. © *2006 American Association of Physics Teachers.*
[DOI: 10.1119/1.2209242]

I. INTRODUCTION

Heterostructures are composite semiconductor structures consisting of two or more layers of different materials deposited alternately on each other.[1] Current technology allows the fabrication of devices consisting of several ultrathin layers which are as thin as one monoatomic layer. Each layer is grown on the previous one reproducing its crystallographic structure, that is, epitaxially, by techniques such as molecular beam epitaxy or metalorganic chemical vapor deposition.[2,3]

Quantum effects play a major role in determining the physical properties of these nanostructured devices, usually referred to as quantum well heterostructures, because the electron mean free paths are usually longer than the layers' thickness. Depending on the number of alternating layers, these devices are single-, double-, or multiple-well heterostructures, where the latter are usually called superlattices. The first fabricated superlattices were crystalline and periodic. It is now possible to build nonperiodic superlattices that are based on amorphous semiconductors.[4] The double-well heterostructures in semiconductor diode lasers are in the majority of compact disc players, laser printers, and fiber optic communication links.[5] Additional applications are found in Refs. 2 and 3.

In the absence of an external electric field, semiconductor superlattices may be considered to be a quasi-one-dimensional system of rectangular quantum wells separated by potential barriers. A standard quantum mechanics analysis of the ballistic transport of electrons through one-dimensional potential wells can describe these devices to a good approximation. To extend the standard solution for the scattering by a quantum well to multiple wells, a transfer matrix method involving the straightforward multiplication of 2×2 matrices has been developed.[6–10] In this paper this method is applied to quasiperiodic superlattices.[11]

The fabrication of these structures is the result of the iterative application of a deterministic set of rules. Their physical properties are between those of stochastic and perfectly periodic superlattices. We will concentrate on fractal superlattices based on generalized Cantor sets.[12]

Fractals are geometric objects that are homogeneous and self-similar and describe naturally occurring fragmented and irregular structures.[13,14] Fractal geometry has been identified in many areas such as biology, medicine, electric circuits, geomorphology, fracture theory, and even stock markets.[15] Mathematical fractals are self-similar structures obtained by performing a basic operation (a generator) on a given geometrical object (the initiator) and repeating this process on multiple levels of detail; at each level an object composed of subunits is created that resembles the structure of the whole object. Mathematically, this property holds on all scales, but in the real world, there are necessarily lower and upper boundaries over which such self-similar behavior applies.

Fractal superlattices based on generalized Cantor sets have been fabricated and measured by x-ray diffraction techniques.[12] These superlattices have been grown by alternating layers of amorphous germanium and amorphous silicon deposited on a silicon substrate such that their layer distribution along the growth axis is identical to the distribution of segments and gaps in a finite order approximation to a Cantor set.

Section II summarizes the transfer matrix method for quantum scattering by piecewise constant potentials. Section III presents the mathematical definition of generalized Cantor sets, their parameters, and the limits imposed on them. In Sec. IV several concepts of the physics of fractal superlattices are briefly reviewed. The main result of this paper is presented in Sec. V, where the reflection coefficient for the tunneling of quantum particles on Cantor superlattices is numerically evaluated. The last section is devoted to the main conclusions, suggestions for the use of the results of this paper in a pedagogical context, and topics for further research.

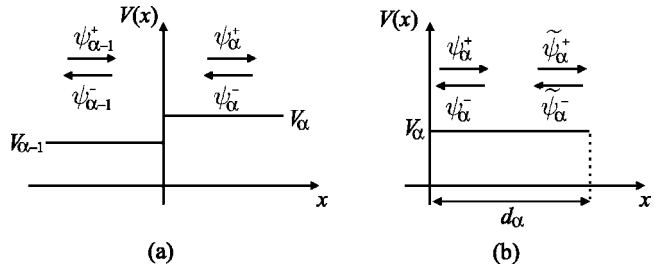

Fig. 1. Notation for the wave functions for (a) scattering with interface α of the piecewise constant potential among the values $V_{\alpha-1}$ and V_α and (b) the propagation through each constant potential V_α.

II. THE TRANSFER MATRIX METHOD

The scattering of particles by one-dimensional potential wells is governed by the time-independent Schrödinger equation

$$-\frac{\hbar^2}{2m}\frac{\partial^2\psi(x)}{\partial^2 x}+V(x)\psi(x)=E\psi(x), \tag{1}$$

where $\psi(x)$, m, and E are the particle wave function, mass and energy, respectively, $\hbar$ is Planck's constant, and $V(x)$ describes a distribution of potential wells. From here on $V(x)$ will be assumed to be a piecewise constant function with N potential wells. We take V_α and d_α to be the potential depth and width, respectively, in well α, with $\alpha=1,2,\ldots,N$. The boundary potential values are designated as V_0 and V_{N+1} for completeness.

The solution of the scattering problem by a piecewise constant potential may be obtained by the transfer matrix method[6–10,16] as follows. Let us start with the simplest setting. Figure 1(a) shows the scattering at interface α between two successive values of the piecewise potential, whose position, without loss of generality, has been taken as $x=0$. As shown in Fig. 1(a), the wave function ψ_α in the region where the constant potential has a value V_α is the sum of two plane waves, $\psi_\alpha(x)=\psi^+_\alpha(x)+\psi^-_\alpha(x)$, given by

$$\psi^\pm_\alpha(x)=A^\pm_\alpha e^{\pm ik_\alpha x},\quad k_\alpha=\frac{1}{\hbar}\sqrt{2m(E-V_\alpha)}, \tag{2}$$

where $i=\sqrt{-1}$, $\hbar k_\alpha$ is the local particle momentum, and $A^\pm_\alpha$ are integration constants to be determined by requiring the continuity of both the wave function and its derivative at the interfaces between successive wells,

$$\psi_{\alpha-1}(x=0)=\psi_\alpha(x=0),\quad A^+_{\alpha-1}+A^-_{\alpha-1}=A^+_\alpha+A^-_\alpha, \tag{3a}$$

$$\psi'_{\alpha-1}(x=0)=\psi'_\alpha(x=0),$$
$$k_{\alpha-1}A^+_{\alpha-1}-k_{\alpha-1}A^-_{\alpha-1}=k_\alpha A^+_\alpha-k_\alpha A^-_\alpha, \tag{3b}$$

where the prime denotes differentiation. These conditions may be written as a 2×2 linear system of equations given by

$$\begin{pmatrix}1 & 1\\ k_{\alpha-1} & -k_{\alpha-1}\end{pmatrix}\begin{pmatrix}A^+_{\alpha-1}\\ A^-_{\alpha-1}\end{pmatrix}=\begin{pmatrix}1 & 1\\ k_\alpha & -k_\alpha\end{pmatrix}\begin{pmatrix}A^+_\alpha\\ A^-_\alpha\end{pmatrix}, \tag{4}$$

which can be expressed in matrix notation as

$$\begin{pmatrix}A^+_{\alpha-1}\\ A^-_{\alpha-1}\end{pmatrix}=D^{-1}_{\alpha-1}D_\alpha\begin{pmatrix}A^+_\alpha\\ A^-_\alpha\end{pmatrix}, \tag{5a}$$

$$D_\alpha=\begin{pmatrix}1 & 1\\ k_\alpha & -k_\alpha\end{pmatrix}. \tag{5b}$$

The matrix $D^{-1}_{\alpha-1}D_\alpha$ is the wave scattering matrix.

Figure 1(b) shows that the plane wave function, after crossing interface α, propagates through the constant potential V_α until the next step at the distance d_α. We use the notation in Fig. 1(b) and write the propagating wavefunction as

$$\tilde{\psi}^\pm_\alpha=A^\pm_\alpha e^{\pm ik_\alpha d_\alpha}e^{\pm ik_\alpha x}=\tilde{A}^\pm_\alpha e^{\pm ik_\alpha x}, \tag{6}$$

which may be written in matrix form as

$$\begin{pmatrix}\tilde{A}^+_{\alpha-1}\\ \tilde{A}^-_{\alpha-1}\end{pmatrix}=P_\alpha\begin{pmatrix}A^+_\alpha\\ A^-_\alpha\end{pmatrix}, \tag{7a}$$

$$P_\alpha=\begin{pmatrix}e^{ik_\alpha d_\alpha} & 0\\ 0 & e^{-ik_\alpha d_\alpha}\end{pmatrix}. \tag{7b}$$

The matrix P_α is known as the wave propagation matrix.

The iterative application of the scattering and propagation matrices may be used to solve the general problem of the scattering by a potential with N wells. The first step is

$$\begin{pmatrix}A^+_0\\ A^-_0\end{pmatrix}=D^{-1}_0D_1\begin{pmatrix}A^+_1\\ A^-_1\end{pmatrix}=D^{-1}_0D_1P_1D^{-1}_1D_2\begin{pmatrix}A^+_2\\ A^-_2\end{pmatrix}, \tag{8}$$

which may be easily generalized to yield

$$\begin{pmatrix}A^+_0\\ A^-_0\end{pmatrix}=M\begin{pmatrix}A^+_{N+1}\\ A^-_{N+1}\end{pmatrix}, \tag{9}$$

$$M=D^{-1}_0\left(\prod_{\alpha=1}^{N}D_\alpha P_\alpha D^{-1}_\alpha\right)D_{N+1}, \tag{10}$$

which corresponds to the solution of Eq. (1) for a distribution of N constant potential wells. We state without proof that M is always a special unitary matrix, that is, $\det(M)=1$, $M_{22}=M^*_{11}$, and $M_{12}=M^*_{21}$. Proofs and further properties may be found in Ref. 8.

The reflection and transmission coefficients for the scattering of a particle incoming from the left by the N-well potential are determined by the coefficients of the matrix M,

$$\begin{pmatrix}A^+_0\\ A^-_0\end{pmatrix}=\begin{pmatrix}M_{11} & M_{12}\\ M_{21} & M_{22}\end{pmatrix}\begin{pmatrix}A^+_{N+1}\\ 0\end{pmatrix}. \tag{11}$$

Because no backward particle can be found on the right side of the potential, $A^-_{N+1}=0$. The reflection and transmission coefficients are given by

$$R=\frac{|A^-_0|^2}{|A^+_0|^2}=\frac{|M_{21}|^2}{|M_{11}|^2}, \tag{12a}$$

$$T=\frac{k_{N+1}|A^+_{N+1}|^2}{k_0|A^+_0|^2}=\frac{1}{|M_{11}|^2}. \tag{12b}$$

Because $V_0=V_{N+1}$, we have $k_{N+1}=k_0$.

The transfer matrix method may be straightforwardly implemented in a computer program, making possible the efficient calculation of the reflection and transmission coefficients of electrons in arbitrary piecewise constant poten-

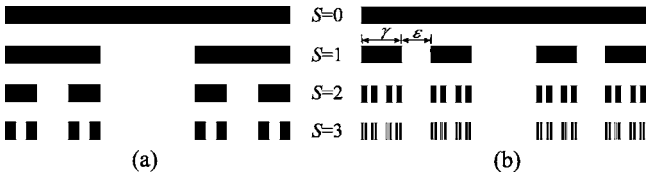

Fig. 2. First steps of development of (a) triadic and (b) polyadic, $N=4$, symmetrical generalized Cantor sets. Black and white regions denote the potential values $-V$ and 0, respectively. The right plot also shows the definition of the scale factor γ and the lacunarity parameter ε characterizing polyadic Cantor sets.

tials. In the remainder of this paper, a distribution of potential wells of the same depth is considered, so $V_\alpha=-V$ in the wells, $V_\alpha=0$ outside them, and $V_0=V_{N+1}=0$.

III. GENERALIZED CANTOR SETS

Generalized Cantor sets[13,17] are the result of removing parts of a finite segment according to an iterative procedure. The simplest is the triadic Cantor set shown in Fig. 2(a), which can be obtained by the following iterative construction. The zeroth step ($s=0$) is to consider a segment of unit length. In the next step ($s=1$) divide the segment into three equal parts of length 1/3 and remove the middle part. In general, at step s there are 2^s segments of length 3^{-s} with 2^s-1 gaps in between. Step $s+1$ is obtained by dividing each of these segments into three parts of length 3^{-s-1} and removing the central ones. In Fig. 2(a) only the first four steps are shown for clarity. Strictly speaking the Cantor set is the limit of this procedure for $s\to\infty$, which is composed of points distributed such that each point lies arbitrarily close to other points in the set.

The main properties of fractal sets are their self-similarity, that is, they appear identical or similar at different scales of magnification, and their fractal dimension, which is a noninteger real number in general. The self-similarity of the triadic Cantor set is evident from its construction. There are several inequivalent definitions of the fractal dimension. The similarity dimension, also referred to as the limit capacity, is the most widely used because it can be computed by simple procedures such as box counting algorithms.[18] For the triadic Cantor set the similarity dimension is $\ln 2/\ln 3=0.63093\ldots$, because every segment is divided into three parts from which only two are retained.

The construction of the triadic Cantor set may be generalized by dividing each segment into more than three parts yielding the symmetrical polyadic Cantor fractal sets.[19,20] The initiator (step $s=0$) is again a straight line segment of unit length. At step $s=1$ the initiator is replaced by N nonoverlapping copies of the initiator, each one scaled by a factor $\gamma<1$. For even N, as shown in Fig. 2(b), one half of the copies are placed to the left of the interval and the other half to its right, each copy being separated by a fixed distance ε. For odd N, not shown in Fig. 2, one copy lies centered in the interval and the rest are distributed as for even N, that is, $\lfloor N/2\rfloor$ copies are placed to the left of the interval and the other $\lfloor N/2\rfloor$ copies to its right, where $\lfloor N/2\rfloor$ is the greatest integer less than or equal to $N/2$. At each step of the construction, the generation process is repeated over and over again for each segment in the previous step.

In general, fractals are not uniquely characterized by their similarity dimension. The similarity dimension of all polyadic Cantor fractal sets is $\ln N/\ln \gamma^{-1}=-\ln N/\ln \gamma$, which is independent of the width of the outermost gap ε at the first step. Hence, further measures of the fractal set may be introduced. The simplest such measure is the lacunarity,[19] which may be defined as the deviation of a fractal from translational invariance.[21] Translational invariance is highly scale dependent because heterogeneous sets at small scales can be homogeneous on larger scales or vice versa. Lacunarity is a scale-dependent measure of the heterogeneity (or texture) of an object, whether or not it is fractal. For the purposes of this paper a rigorous definition of the mathematical concept of lacunarity is not necessary, and it is sufficient to consider ε as an indication of the lacunarity of the generalized Cantor set, as shown in Fig. 3. This parameter is inversely related to lacunarity (the highest lacunarity is obtained for the minimum value of ε), so it is not a good measure of lacunarity. However, as in most papers dealing with polyadic Cantor fractals in physics and engineering applications,[20,22] ε is chosen as the simplest parameter representing the lacunarity. Therefore, we will refer to ε as the lacunarity parameter.

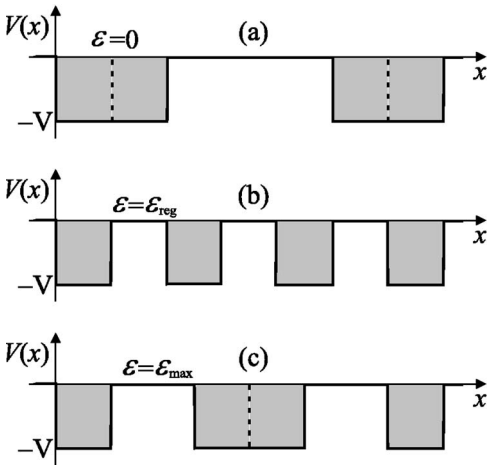

Fig. 3. Potential wells for $\varepsilon=0$ (a), $\varepsilon_{\rm reg}$ (b), and $\varepsilon_{\max}$ (c) for a polyadic Cantor set potential with $N=4$ and $s=1$.

Symmetrical polyadic Cantor fractals are characterized by the number of self-similar copies N, the scaling factor γ, and the lacunarity parameter ε. The last two parameters must satisfy certain constraints to avoid overlapping between the copies. The maximum value of the scaling factor depends on the value of N, such that $0<\gamma<\gamma_{\max}=1/N$. For each value of N and γ, there are two extreme values for ε. One is $\varepsilon_{\min}=0$, see Fig. 3(a), for which the highest lacunar fractal is obtained, that is, one with the largest possible gap. For even N, the central gap has a width of $1-N\gamma$, and for odd N, both large gaps surrounding the central well have a width of $(1-N\gamma)/2$. The other extreme value is

$$\varepsilon_{\max}=\begin{cases}\dfrac{1-N\gamma}{N-2} & \text{even } N\\[2ex] \dfrac{1-N\gamma}{N-3} & \text{odd } N,\end{cases} \tag{13}$$

where for even (odd) N two (three) wells are joined together in the center and the central gap is missing, see Fig. 3(c). The width of the $N-2$ gaps in this case is equal to $\varepsilon_{\max}$. Thus the corresponding lacunarity is smaller than that for $\varepsilon=0$, but not the smallest one, which is obtained for the most regular dis-

tribution, where the gaps and wells have the same width at the first step ($s=1$) given by

$$\varepsilon_{\text{reg}} = \frac{1-N\gamma}{N-1}, \tag{14}$$

see Fig. 3(b). Note that $0<\varepsilon_{\text{reg}}<\varepsilon_{\max}$.

IV. CANTOR FRACTAL SUPERLATTICES

We briefly review some elementary concepts of solid-state physics. In a solid the atomic energy levels evolve into (essentially continuous) energy bands. The valence band is the highest energy band filled with electrons and the conduction band is the next higher band (partially empty). The energy states between them are not allowed and are referred to as the band gap, whose width is the band gap energy. When two materials whose band gap energies are different are sandwiched, an attractive potential well is formed for the electrons in the valence band, yielding a quantum well. This finite potential well is thinner in the growth (say vertical) direction than in the transverse directions. Therefore the system may be considered as a two-dimensional system in the transverse directions, where electrons behave as a two-dimensional free electron gas with continuous energy states, and a one-dimensional finite square well in the growth direction, where electrons have discrete bound states.

The electrons in the heterostructure do not respond as free particles when an external force is applied due to the influence of the regular distribution of the atoms of the semiconductor materials. These effects can be taken into account by introducing an effective mass that relates the particle motion to an external force (or potential) without worrying about all the atomic forces. For example, an electron in the conduction band of silicon (Si), germanium (Ge), and gallium arsenide (GaAs) responds as if its effective mass is, respectively, 0.98, 1.64, and 0.067 times the (vacuum) electron mass.[23] The transfer matrix method may be applied to the study of the scattering of electrons by a multiwell piecewise constant potential if the effective mass concept is incorporated.

Superlattices may be periodic, as first suggested by Esaki and Tsu in 1970, random, or quasiperiodic, depending on the distribution of the thickness of the alternating layers.[4] Semiconductor superlattices may be either crystalline or amorphous. A typical crystalline device is made by alternating layers of GaAs and aluminum gallium arsenide ($Al_xGa_{1-x}As$, whose crystal composition x may vary between 0 and 1). These layers are grown epitaxially, that is, the atoms are in registry, with a thickness of only a few nanometers. For example, for $x=0.3$ a monolayer of $Al_xGa_{1-x}As$ has a thickness of 0.28 nm.[24] A typical amorphous device is made by alternating layers of amorphous germanium (a-Ge) and amorphous silicon (a-Si) deposited on a silicon substrate.[12] In such a case, each layer can have a thickness of less than 1.4 nm with very sharp boundaries.

In Cantor superlattices the distribution of the layers' thickness along the growth axis is identical to the distribution of segments and gaps in any finite order approximation to a polyadic Cantor set. Generalized Cantor superlattices have been grown experimentally by alternating layers of a-Ge and a-Si up to the fifth generation of the triadic Cantor set, that is, 3^6 (729) elementary layers were used resulting in a total thickness of 1020.6 nm.[12] The experimental results show that the biggest imperfections, small layer thickness fluctuations and interface mixing, mainly influence the peak intensity, and the relative peak positions are much less affected.[12] In this paper we will neglect the effects due to fabrication imperfections to simplify the analysis.

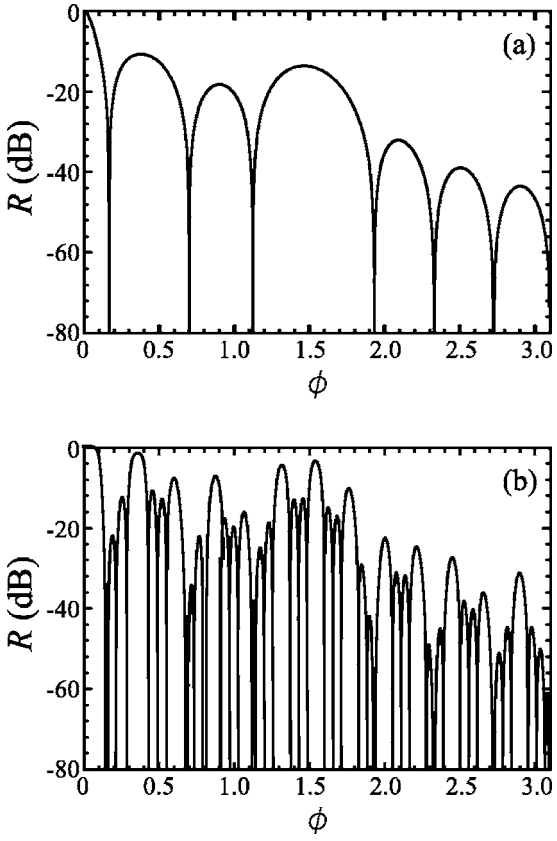

Fig. 4. Scattering reflection coefficient for the polyadic Cantor prefractal potentials with (a) $s=1$ and (b) $s=2$ with $N=4$, $\gamma=1/7$, and $\phi_V=1/2$.

V. RESULTS

The scattering problem for polyadic Cantor sets with variable lacunarity can be solved by the transfer matrix method. We focus on the influence of the lacunarity on the reflection coefficient.[25] We assume that the lacunarity parameter is continuous, although in reality it is an integer multiple of the ratio between the thickness of the monoatomic layers of both semiconductor materials used in the fabrication process of the superlattice.

We normalize both the energy and the depth of the potential wells by their width at the sth step, and let $a=L\gamma^s$, where L is the length of the initiator. We use the dimensionless variables

$$\phi = a\frac{\sqrt{2mE}}{\hbar}, \quad \phi_V = a\frac{\sqrt{2m\tilde{V}}}{\hbar}, \tag{15}$$

where m is the electron effective mass in the material used for the Cantor gaps in the superlattice (a-Si in Ref. 12), $\tilde{V}=m^*\,\text{V/m}$, V is the potential at the wells, and m^* is the electron effective mass in the material corresponding to the Cantor segments (a-Ge in Ref. 12).

Figure 4 shows the reflection coefficient in decibels ($10\log_{10}R$) for tetradic ($N=4$) Cantor potential wells with $s=1$ (a) and $s=2$ (b) for $\gamma=1/7$ and $\phi_V=1/2$. The horizontal

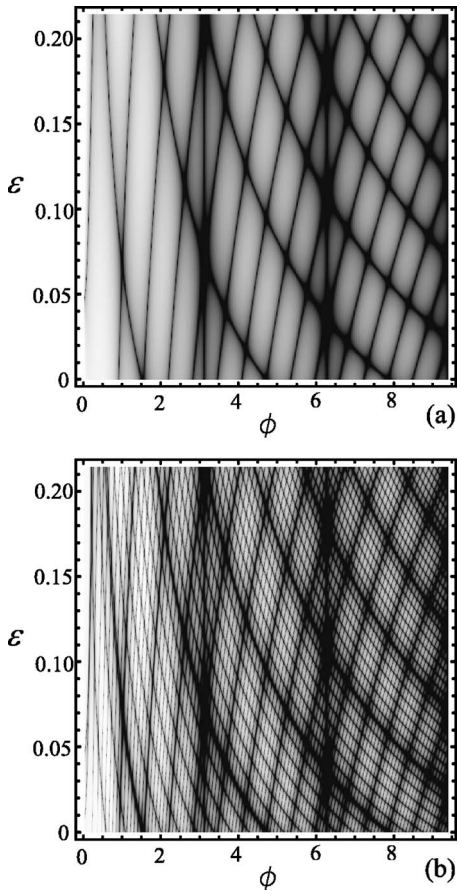

Fig. 5. Twist plots, that is, gray-scale representation of the scattering reflection coefficient (in decibels) as a function of the normalized energy ϕ and the lacunarity parameter ε for the polyadic Cantor prefractal potentials with (a) $s=1$ and (b) $s=2$, for $N=4$, $\gamma=1/7$, and $\phi_V=1/2$.

axis covers the normalized energy ϕ from 0 to $\sqrt{\pi^2-\phi_V^2}\approx 3.10$, for which $R=0$, referred to as the first vertical zero line for reasons to be given in the following. Figure 4 shows that the reflection spectrum exhibits a characteristic fractal profile reproducing the self-similarity of the potential distribution. A wide peak at step s is replaced by several narrower and higher peaks at step $s+1$. The zeros of the reflection coefficient shown in Fig. 4 correspond to resonances of the particle in subsets of wells of the fractal potential. The correlation function of the reflection function with scaled versions of itself shows its self-similarity as done in Ref. 16 for triadic Cantor superlattices.

To show that the self-similar behavior of the reflection coefficient for polyadic Cantor potentials is retained even when the lacunarity parameter is varied, twist plots[20] may be used. These plots represent the reflection coefficient in decibels as a function of the normalized energy ϕ and the lacunarity parameter ε. Figure 5 shows twist plots for tetradic ($N=4$) Cantor potential wells for $s=1$ (a) and $s=2$ (b). In these plots a linear gray scale was used for the reflection coefficient, from black for zero values to white for the maximum value equal to unity. The most noticeable feature of Fig. 5 is the black lines corresponding to energies at which the particle transparently tunnels through the fractal potential wells, that is, for which the reflection coefficient is zero. The horizontal axis covers the first three vertical zeros, that is, $\phi\in[0,\sqrt{(3\pi)^2-\phi_V^2}]\approx[0,9.41]$. These zeros can be calculated from first principles as was done for the interference of light in dielectric fractal superlattices.[20]

The vertical zeros are located at the values ϕ_α given by

$$\phi_\alpha=\sqrt{(\alpha\pi)^2-\phi_V^2},\quad \alpha=1,2,\ldots\ . \tag{16}$$

These zeros are caused by the bound states of the particle in each potential well being independent of the lacunarity parameter. A derivation of Eq. (16) is presented in the appendix. Our normalization of the energy makes the position of the vertical zeros independent of both the initiator length and the fractal first step ($s=1$) as shown in Fig. 5.

Figure 5 also shows that the rescaled reflection coefficient at step $s=1$ forms an envelope for the (unscaled) reflection coefficient at $s=2$, both structures being self-similar for any value of ε. This result shows that the scattering by polyadic Cantor fractal potentials has self-similar properties similar to those reported for triadic Cantor fractal potentials.[16]

VI. CONCLUSIONS

The pedagogical impact of the introduction of computational tools as a complementary teaching tool in undergraduate physical courses has been discussed by several authors.[26] In quantum mechanics courses the transfer matrix method[6–10] is nearly ideal for assignments in a complementary computational laboratory, because it can be easily derived from an analysis of tunneling through a rectangular barrier without discussing more advanced computational techniques. The transfer matrix method can be applied to potential barriers of arbitrary shape while retaining a transparent connection to the original rectangular barrier problem. To further motivate students, interesting potential configurations can be studied. Fractal quantum potentials based on the Cantor set have been proposed in Ref. 16, where suggestions on how to use this tool in physics courses are also given. The inherent beauty of the fractals shown in this paper and a color presentation of the twist plots are highly motivating for students.

Our experience is based on using additional lectures and MATHEMATICA, which our students already know, although any computational software package or programming language can be used for this task. Different aspects of the model may be assigned to different students or groups of students and discussions among the students follow naturally from this approach. Students generally ask for more advanced tasks on fractals.

For graduate students, the techniques for lacunarity analysis[21] and the comparison of algorithms for the calculation of the lacunarity in disordered potential distributions[27] are possible future research areas.

Because transfer matrix methods can be adapted by analogy to the propagation of waves in general one-dimensional quasiperiodic media,[28] the present results may be also applied to acoustics, optics, and vibrating strings. The effect of lacunarity on the scattering by generalized Cantor media was first studied in optics,[20,22] where the additional degree of freedom introduced by the lacunarity was used with success to obtain new physical properties. A detailed study of these applications, while outside the scope of this paper, would be a stimulating topic for further study.

ACKNOWLEDGMENTS

The authors thank an anonymous referee for his useful comments. This work has been partially supported by Grant Nos. FIS2005-01189 and FIS2005-03191 of the Ministerio de Educación y Ciencia of Spain. We also acknowledge financial support from the Universidad Politécnica de Valencia (Vicerrectorado de Innovación y Desarrollo, Programa de Incentivo a la Investigación 2005), Spain.

APPENDIX: VERTICAL ZEROS OF THE REFLECTION COEFFICIENT

The vertical zeros shown in the twist plots of Fig. 5 are the result of bound states of the particle. Using the matrix method it is easy to calculate their exact positions. For only one quantum well of width a, we take $N=1$ in Eq. (9), with $V_0=V_2=0$, $V_1=-V$, and $d_1=a$. The particle wave number in the three constant potential regions is

$$k_0=k_2=\frac{\sqrt{2mE}}{\hbar}=\frac{\phi}{a}, \tag{A1a}$$

$$k_1=\frac{\sqrt{2m(E+V)}}{\hbar}=\frac{\sqrt{\phi^2+\phi_V^2}}{a}. \tag{A1b}$$

The total scattering matrix is given by

$$M=D_0^{-1}D_1P_1D_1^{-1}D_2=\begin{pmatrix}M_{11} & M_{12}\\ M_{21} & M_{22}\end{pmatrix}, \tag{A2}$$

which can be calculated to obtain

$$M_{11}=M_{22}^*=\cos(ak_1)+i\frac{k_0^2+k_1^2}{2k_0k_1}\sin(ak_1), \tag{A3a}$$

$$M_{12}=M_{21}^*=-i\frac{k_0^2-k_1^2}{2k_0k_1}\sin(ak_1), \tag{A3b}$$

where the asterisk indicates the complex conjugate. The matrix M is unitary, with $\det(M)=|M_{11}|^2+|M_{12}|^2=1$.

Bound states of the particle inside the potential well are characterized by a zero reflection coefficient,

$$R=\frac{|M_{21}|^2}{|M_{11}|^2}=0. \tag{A4}$$

This condition is equivalent to

$$\sin(ak_1)=\sin(\sqrt{\phi^2+\phi_V^2})=0, \tag{A5}$$

having denumerably infinite solutions given by

$$\sqrt{\phi_\alpha^2+\phi_V^2}=\alpha\pi, \quad \alpha=1,2,\ldots, \tag{A6}$$

which results in Eq. (16).

[a]Electronic mail: jmonsori@fis.upv.es

[1] R. M. Kolbas and N. Holonyak, Jr., "Man-made quantum wells: A new perspective on the finite square-well problem," Am. J. Phys. **52**(5), 431–437 (1984).
[2] B. R. Nag, *Physics of Quantum Well Devices* (Kluwer Academic, Dordrecht, 2001).
[3] P. Roblin, *High-Speed Heterostructure Devices: From Device Concepts to Circuit Modeling* (Cambridge U.P., New York, 2002).
[4] R. Mazurczyk, "Semiconductor superlattice," Chaos, Solitons Fractals **10**(12), 1971–1982 (1999).
[5] P. S. Zory, Jr., *Quantum Well Lasers* (Academic, New York, 1993), pp. 1–13.
[6] J. M. Ziman, *Models of Disorder* (Cambridge U.P., Cambridge, 1979), pp. 291–301.
[7] T. M. Kalotas and A. R. Lee, "One-dimensional quantum interference," Eur. J. Phys. **12**(6), 275–282 (1991).
[8] D. W. L. Sprung, H. Wu, and J. Martorrell, "Scattering by a finite periodic potential," Am. J. Phys. **61**(12), 1118–1124 (1993).
[9] J. S. Walker and J. Gathright, "Exploring one-dimensional quantum mechanics with transfer matrices," Am. J. Phys. **62**(5), 408–422 (1994).
[10] G. P. Gilfoyle, "A new teaching approach to quantum mechanical tunneling," Comput. Phys. Commun. **121–122**, 573–577 (1999).
[11] K. J. Chen, G. M. Mao, Z. F. Li, H. Chen, J. F. Du, and X. R. Zang, "Multilayer amorphous semiconductors," Thin Solid Films **163**, 55–60 (1988).
[12] K. Järrendahl, M. Dulea, J. Birch, and J.-E. Sundgren, "X-ray diffraction from amorphous Ge/Si Cantor superlattices," Phys. Rev. B **51**(12), 7621–7631 (1995).
[13] A. J. Hurt, "Resource Letter FR-1: Fractals," Am. J. Phys. **56**(11), 969–975 (1988).
[14] B. B. Mandelbrot, *The Fractal Geometry of Nature* (Freeman, New York 1983).
[15] *Fractals in Biology and Medicine*, edited by T. F. Nonnenmacher, G. A. Losa, and E. R. Weibel (Birkhauser, Berlin, 1994); W. K. Ching, M. Erickson, P. Garik, P. Hickman, J. Jordan, S. Schwarzer, and L. Shore, "Overcoming resistance with fractals: A new way to teach elementary circuits," Phys. Teach. **32**(9), 546–551 (1994); D. L. Turcotte, *Fractals and Chaos in Geology and Geophysics* (Cambridge U.P., Cambridge, 1997), 2nd ed.; F. M. Borodich, "Fractals and fractal scaling in fracture mechanics," Int. J. Fract. **95**(1-4), 239–259 (1999); D. Sornette, *Why Stock Markets Crash: Critical Events in Complex Financial Systems* (Princeton U.P., Princeton, NJ, 2002).
[16] J. A. Monsoriu, F. R. Villatoro, M. J. Marín, J. F. Urchueguía, and P. Fernández de Córdoba, "A transfer matrix method for the analysis of fractal quantum potentials," Eur. J. Phys. **26**(4), 603–610 (2005).
[17] Reference 14, pp. 74–83.
[18] C. Essex and M. A. H. Nerenberg, "Fractal dimension: Limit capacity or Hausdorff dimension?," Am. J. Phys. **58**(10), 986–988 (1990).
[19] Reference 14, pp. 310–318.
[20] A. D. Jaggard and D. L. Jaggard, "Scattering from fractal superlattices with variable lacunarity," J. Opt. Soc. Am. A **15**(6), 1626–1635 (1998).
[21] R. E. Plotnick, R. H. Gardner, W. W. Hargrove, K. Prestegaard, and M. Perlmutter, "Lacunarity analysis: A general technique for the analysis of spatial patterns," Phys. Rev. E **53**(5), 5461–5468 (1996).
[22] J. A. Monsoriu, G. Saavedra, and W. D. Furlan, "Fractal zone plates with variable lacunarity," Opt. Express **12**(18), 4227–4234 (2004).
[23] K. K. Ng, *Complete Guide to Semiconductor Devices* (Schaum's Solved Problems Books, McGraw-Hill, New York, 1995), p. 612.
[24] F. Axel and H. Terauchi, "High-resolution x-ray-diffraction spectra of Thue-Morse GaAs-AlAs heterostructures–Towards a novel description of disorder," Phys. Rev. Lett. **66**(17), 2223–2226 (1991).
[25] The results for triadic Cantor sets have been previously reported in Ref. 16, where the self-similarity of the reflection coefficient for prefractal potentials was qualitatively shown by plots and quantified by means of the correlation function.
[26] R. A. Lewis, B. M. Harper, and M. Wilson, "Computer assignments and problems classes for physics students," Comput. Educ. **16**(4), 349–362 (1991); C. Y. Chang, "Does computer-assisted instruction + problem solving=improved science outcomes? A pioneer study," J. Educ. Res. **95**(3), 143–150 (2002); F. Esquembre, "Computers in physics education," Comput. Phys. Commun. **147**(1-2), 13–18 (2002); R. L. Spencer, "Teaching computational physics as a laboratory sequence," Am. J. Phys. **73**(2), 151–153 (2005).
[27] C. Allain and M. Cloitre, "Characterizing the lacunarity of random and deterministic fractal sets," Phys. Rev. A **44**, 3552–3558 (1991).
[28] D. J. Griffiths and C. A. Steinke, "Waves in locally periodic media," Am. J. Phys. **69**(2), 137–154 (2001).